

Acceleration of 1I/‘Oumuamua from radiolytically produced H₂ in H₂O ice

Jennifer B. Bergner^{1,2} & Darryl Z Seligman³

¹*University of California, Berkeley, Department of Chemistry, Berkeley, CA 94720, USA; email: jbergner@berkeley.edu; ORCID: 0000-0002-8716-0482*

²*University of Chicago Department of the Geophysical Sciences, Chicago, IL 60637, USA*

³*Department of Astronomy and Carl Sagan Institute, Cornell University, 122 Sciences Drive, Ithaca, NY, 14853, USA; email: dzs9@cornell.edu; ORCID: 0000-0002-0726-6480*

In 2017, 1I/‘Oumuamua was identified as the first known interstellar object in the Solar System¹. Although typical cometary activity tracers were not detected²⁻⁶, ‘Oumuamua exhibited a significant non-gravitational acceleration⁷. To date there is no explanation that can reconcile these constraints⁸. Due to energetic considerations, outgassing of hyper-volatile molecules is favored over heavier volatiles like H₂O and CO₂⁹. However, there are theoretical and/or observational inconsistencies¹⁰ with existing models invoking the sublimation of pure H₂⁹, N₂,¹¹ and CO¹². Non-outgassing explanations require fine-tuned formation mechanisms and/or unrealistic progenitor production rates^{7,13-15}. Here we report that the acceleration of ‘Oumuamua is due to the release of entrapped molecular hydrogen which formed through energetic processing of an H₂O-rich icy body. In this model, ‘Oumuamua began as an icy planetesimal that was irradiated at low temperatures by cosmic rays during its interstellar journey, and experienced warming during its passage through the Solar System. This explanation is supported by a large body of experimental work showing that

H₂ is efficiently and generically produced from H₂O ice processing, and that the entrapped H₂ is released over a broad range of temperatures during annealing of the amorphous water matrix^{16–22}. We show that this mechanism can explain many of ‘Oumuamua’s peculiar properties without fine-tuning. This provides further support³ that ‘Oumuamua originated as a planetesimal relic broadly similar to Solar System comets.

After the identification of ‘Oumuamua as an interstellar object, extensive follow-up studies revealed it to host a featureless red reflection spectrum^{2–5}, no detectable dust or gas coma^{2,4,6}, an extreme 6:6:1 geometry^{2,4,23}, and a low inbound galactic velocity dispersion implying a young $\lesssim 100$ Myr age^{8,24,25}. Considering these constraints, together with the observed non-gravitational acceleration⁷, we propose that ‘Oumuamua originated as an H₂O-rich icy planetesimal that was ejected from its formation system and underwent energetic processing in the cold interstellar medium. This bombardment by cosmic rays and high energy photons produced entrapped H₂ that was released upon thermal annealing of the H₂O matrix during its passage through the Solar System. This model does not require a fine-tuned formation scenario, and reconciles the observations that (i) the surface properties of ‘Oumuamua are consistent with some Solar System comets, (ii) spectroscopically active gases were not detected, and (iii) the body nonetheless exhibited non-gravitational acceleration. Note that H₂ would not be detectable from the spectroscopic observations of ‘Oumuamua at optical, centimeter, and IR wavelengths which were used to provide upper limits on the production rates of other gases^{5,6,26}.

The processing of H₂O ice in astrophysically relevant conditions has been extensively ex-

plored with laboratory experiments. H_2 formation from H_2O processing (or D_2 from D_2O) has been demonstrated for various energy sources (energetic particles, UV photons, electrons), water structures (crystalline and amorphous), and compositions (water ice that is both pure and doped with other volatiles)^{16–22}. Of relevance to the highly porous structure of comet-like bodies, H_2 production has been shown to increase along with ice porosity^{19,22}. The majority of H_2 produced from in situ ice processing at low temperatures (~ 10 K) remains trapped within the water matrix until the ice is heated to temperatures ranging from 15 to 140 K^{17,20}.

Non-gravitational acceleration of some form is required to match the 207 astrometric observations of ‘Oumuamua collected when it was between 1.2–2.8 au^{7,12}. The best fit to the non-gravitational acceleration is primarily in the anti-solar direction with an r^{-1} or r^{-2} radial dependency. During this time (and specifically during the first 6 October nights when high temporal cadence photometric data were obtained) the lightcurve was used to infer object dimensions of $115 \times 111 \times 19$ meters, though the size is degenerate with the geometric albedo²³ (the quoted dimensions assume an albedo of 0.1). Before this time, it is unknown whether ‘Oumuamua experienced non-gravitational acceleration and what its shape or size may have been.

$\text{H}_2/\text{H}_2\text{O}$ yields as high as 35% have been measured in experiments of H_2O ice processing¹⁷. $\text{H}_2/\text{H}_2\text{O}$ yields of tens of percent are predicted for the top few meters of a cometary body exposed to galactic cosmic rays (GCRs)²⁷. Indeed, GCRs are the most relevant energy source for this scenario since they can penetrate to depths of tens of meters into an icy body²⁸. Moreover, in the solar system, the $\text{H}/(\text{C}+\text{O})$ ratio in volatile cometary material is ~ 1.6 , compared to a ratio of ~ 0.5

in refractory organic material^{29,30}. This implies that a majority of the original H content can be lost during chemical processing of volatile ice mixtures. Based on the above lines of evidence, it is reasonable to assume that H₂/H₂O yields in the low tens of percent can be achieved for the top several meters of an irradiated comet-like body. In our model we test uniform fixed H₂/H₂O ratios of 0.3 and 0.4 throughout the body, corresponding to conversion yields H₂(final)/H₂O(initial) of ~20–30%.

In order to be a feasible accelerant, H₂ outgassed from the surface layers of ‘Oumuamua must provide sufficient force to explain the observed non-gravitational acceleration. To test this model, we calculate the number of H₂ molecules in an outgassing shell on the surface of the ellipsoidal body ($N_{\text{H}_2,\text{shell}}$), and compare this to the total number of molecules required to explain the non-gravitational acceleration ($N_{\text{H}_2,\text{accel}}$) (Methods; Equation 6). When $N_{\text{H}_2,\text{shell}} / N_{\text{H}_2,\text{accel}} > 1$, the model is feasible. This fraction depends on several parameters which are unconstrained for ‘Oumuamua: the albedo (and corresponding size) of the body, the outgassing depth, the temperature of the outgassing H₂, the geometry of outflowing gas (e.g. collimated vs. isotropic), the H₂/H₂O ratio, and the water/dust mass ratio. We therefore explore a range of values reasonable for a comet-like body, described in the Methods section. Figure 1 demonstrates that the feasibility criterion is satisfied for a wide range of the expected parameter space in both optimistic and conservative cases.

We next perform thermal modeling of ‘Oumuamua (Methods) to determine whether the object could produce H₂ from the depths implied by Figure 1. Experiments have demonstrated that

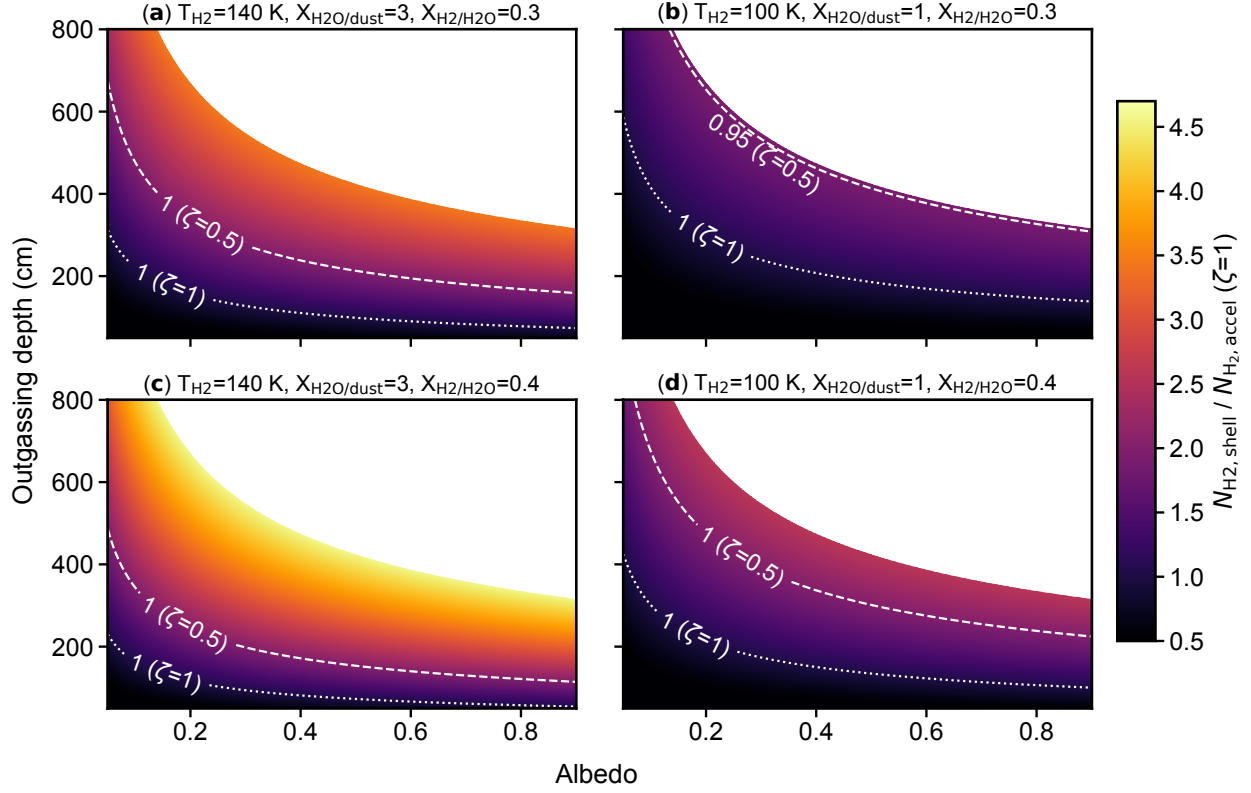


Figure 1: The model feasibility for a range of possible parameter space. The model is feasible when $N_{\text{H}_2,\text{shell}}/N_{\text{H}_2,\text{accel}} > 1$, i.e. the number of H_2 molecules in an outgassing shell is sufficient to explain the observed non-gravitational acceleration between 1.2–2.8 au. Each panel shows this ratio for a range of geometric albedos and outgassing depths. The white regions represent unphysical combinations of albedo and outgassing depth ($d > r_c$). Different assumptions for the outflow temperature, $\text{H}_2\text{O}/\text{dust}$ mass ratio, and $\text{H}_2/\text{H}_2\text{O}$ number density ratio are shown in Panels A-D. Lines show where the ratio is 1 for the case of a collimated outflow (dotted, $\zeta=1$) and an entirely isotropic hemispherical outflow (dashed, $\zeta=0.5$). Regions above these contours represent allowable parameter space for a given set of assumptions. In panel B the dashed line corresponds to a ratio of 0.95, the maximum reached for that $\zeta=0.5$ scenario. Colormaps correspond to the $\zeta=1$ case for each panel.

H₂ is released from within an amorphous H₂O ice matrix between 15–140 K, first due to sublimation of H₂ from channels with access to the surface (<30 K), and then due to annealing of the H₂O ice which causes micropores and macropores to collapse^{19,22,31}. The fractions released within different temperature regimes have been estimated at 2/3 from 15–30 K, 1/9 from 30–80 K, and 2/9 from 80–140 K³², though this may differ in ices of cometary thickness compared to the experiments. Based on these experiments, we expect H₂ outgassing to be active for comet layers that are warmed to ~15–140 K. Figure 2 shows the simulated radial temperature profile of ‘Oumuia over the course of the observations. We show the temperature profile for two end member values of the thermal conductivity³³. For a low thermal conductivity, temperatures of 15–140 K are reached between 50–250 cm below the surface, while for a higher thermal conductivity the necessary temperatures are reached down to ~8 meters. It is possible that additional heating may be produced from the exothermicity of crystallization or annealing of the water matrix³⁴. Upon comparison with Figure 1, it is clear that the nucleus can be warmed to sufficient depths to explain the necessary extent of H₂ outgassing (e.g. 200–400 cm for moderate albedos).

Our thermal models predict that surface temperatures greater than the water sublimation temperature (~150 K) can be reached interior to 3 au. While it has been shown that H₂O alone could not provide sufficient non-gravitational acceleration due to energetic constraints^{9,35}, spectroscopic observations did not rule out H₂O outgassing. Indeed, upper limits from radio lines of OH (a dissociation product of H₂O) with the Green Bank Telescope correspond to an upper limit on the water mass loss rate of $\dot{M} \leq 30 \text{ kg s}^{-1}$ at 1.8 au^{8,26}, which is considerably higher than the production that would be needed to power the non-gravitational acceleration⁷. If H₂O sublimation was active, this

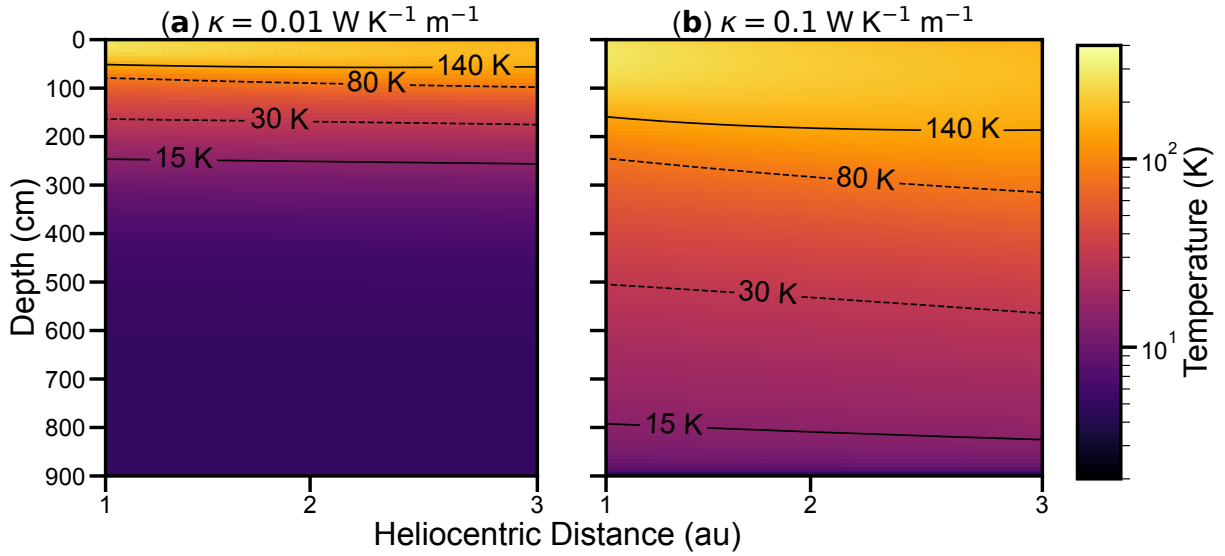


Figure 2: Thermal model of ‘Oumuamua during the observational arc where non-gravitational acceleration is required. We adopt a bulk density $\rho_{Bulk} = 0.5 \text{ g cm}^{-3}$, specific heat capacity of $c_P = 2000 \text{ J kg}^{-1} \text{ K}$ and thermal conductivity $\kappa = 10^{-2} \text{ W K}^{-1} \text{ m}$ (panel A) and $\kappa = 10^{-1} \text{ W K}^{-1} \text{ m}$ (panel B). H_2 outgassing is expected for temperatures of $\sim 15\text{--}140 \text{ K}$.

would lower the required yields of H_2 needed to explain the non-gravitational acceleration. Based on the energetic constraints from ⁹, H_2O sublimation could explain at most $\sim 50\%$ of the observed non-gravitational acceleration. Alternatively, H_2O may not have been present near the surface due to the formation of a low-conductivity regolith during interstellar radiation processing^{3,4,36}. In any case, we have demonstrated that radiolytically produced H_2 could provide the non-gravitational acceleration of ‘Oumuamua despite the ambiguity regarding H_2O production.

Our modeling approach is necessarily simple owing to a dearth of quantitative constraints. Additional laboratory efforts are needed to enable a more sophisticated treatment. In particular, we stress the need to robustly establish the yields of H_2 from different types and doses of energetic processing, both for pure H_2O ice and comet-like volatile ice mixtures. This also includes measuring the H_2 fraction that escapes in different temperature regimes for different ice thicknesses. Better descriptions of the energetics and kinetics of amorphous H_2O ice annealing are also needed.

A remaining obstacle to any outgassing-based explanation for ‘Oumuamua’s non-gravitational acceleration is the upper limit on the reported (and model-dependant) μm sized dust production ($\dot{M} \leq 2 \times 10^{-4} - 2 \times 10^{-3} \text{ kg s}^{-1}$), which is lower than expected based on active solar system comets^{2,4}. Micheli et al.⁷ posit that the dust from ‘Oumuamua could have been released as larger grains ($> 100 \mu\text{m}$), and also note that small dust activity is not universal in solar system comets³⁷. For example, the well studied comet 2P/Encke is notoriously underabundant in small dust particles³⁸, though this may be due to thermal processing within the inner solar system. We expand upon these arguments by considering μm sized dust that is initially on the surface of the object or trapped

within the subsurface ice matrix. It has been demonstrated that interactions with ambient gas in the interstellar medium preferentially remove small dust grains from the surface of long-period comets and interstellar comets³⁹. Furthermore, ‘Oumuamua is considerably smaller than any active comet detected to date in the solar system⁸. It is possible that smaller objects with weaker self gravity are less efficient at retaining surface dust particles. Indeed, the lack of known small Solar System comets could reflect an observational bias due to intrinsically lower dust production rates. In the scenario proposed here, we further note that H₂ is less massive than other volatiles associated with cometary activity (e.g. 2 vs. 28 m_H for H₂ vs. CO). Therefore, H₂ production will provide considerably less momentum for entraining dust either from the surface or within the ice matrix. Similarly, it is plausible that H₂O annealing will release entrapped H₂ while the primordial dust remains bound in the ice matrix. Improved constraints on the efficiency of small dust entrainment in the outgassing of different hypervolatiles are important not only for ‘Oumuamua but for interpreting cometary activity more generally.

The model proposed here is generic and implies that all icy bodies exposed to sufficient high energy radiation should exhibit some degree of H₂O conversion to H₂. This process should be particularly efficient for Oort Cloud comets that are not shielded from cosmic rays by the heliosphere. It is important to note the small size of ‘Oumuamua, which is at least an order of magnitude smaller than solar system comets with ‘classic’ activity (e.g. spectroscopically active volatiles and/or small dust; see Figure 5 in⁸). Because ice processing will be most efficient in the top few meters of the surface of a comet²⁷, the outgassing of H₂ from a larger, more massive body should not be expected to produce a meaningful acceleration. Therefore, it is likely that the detection of non-gravitational

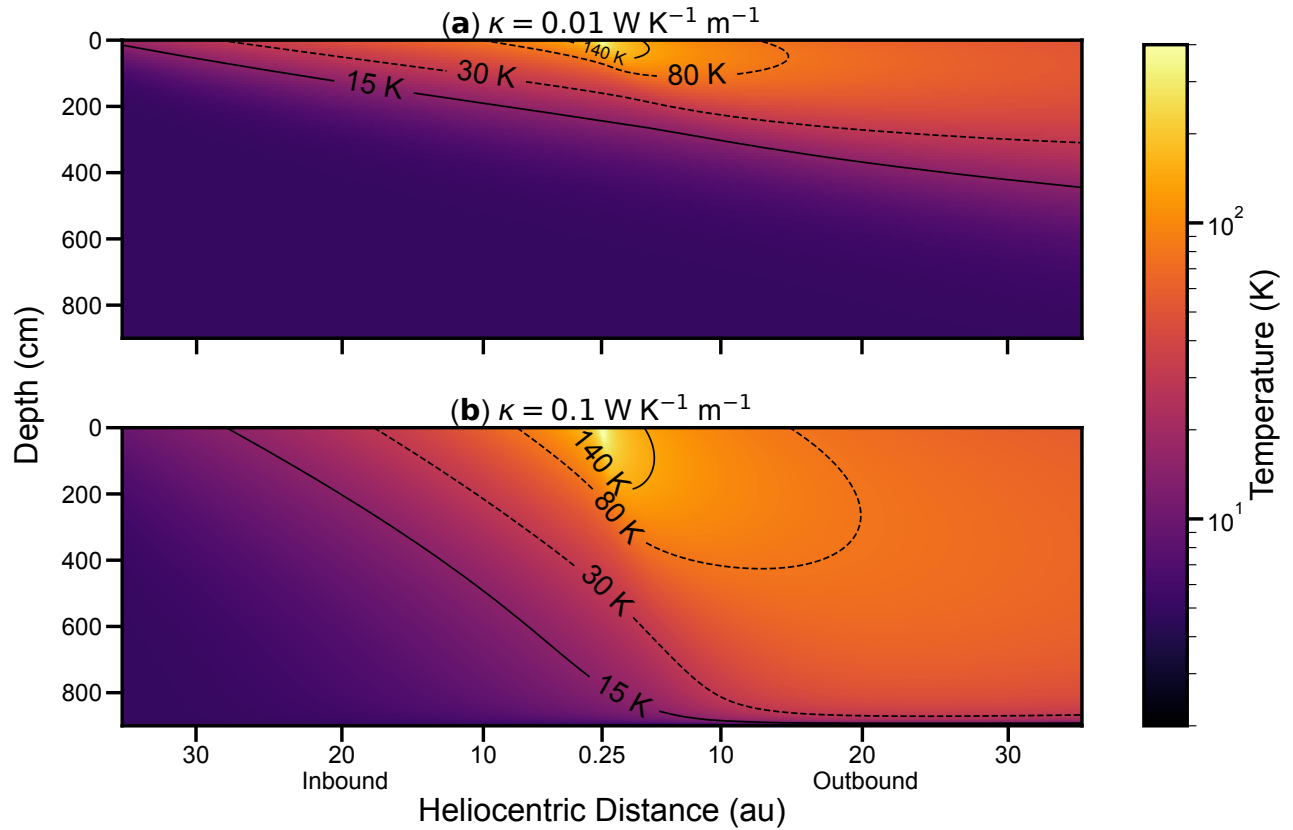


Figure 3: Thermal model of ‘Oumuamua over the course of the entire trajectory interior to the orbit of Neptune. Adopted parameters are the same as in Figure 2.

acceleration of ‘Oumuamua was possible owing to its small size.

A prediction of our model is that small long-period and interstellar comets should exhibit non-gravitational accelerations analogous to ‘Oumuamua as they approach the Sun, even if they exhibit faint or non-detectable activity. Figure 3 shows the thermal profile of an object on the same trajectory as ‘Oumuamua to distances past Neptune. Based on this model, H_2 outgassing from the surface layers of icy bodies may begin at large heliocentric distances (e.g. outgassing down to 2

meters between 10–20 au). Follow-up observations of small solar system bodies and interstellar objects discovered with the Rubin Observatory Legacy Survey of Space and Time (LSST) will therefore enable the proposed mechanism to be tested. Future detections of small bodies with non-gravitational acceleration and faint coma could provide insights into the origins of ‘Oumuamua even though it has long departed the Solar System.

Methods

H₂ budget We first calculate the total number of H₂ molecules needed to explain the non-gravitational acceleration between 1.2–2.8 au. Following the fits of ⁷, we assume the acceleration as a function of heliocentric distance r is described by $a(r)=4.92\times 10^{-6}\left(r/1\text{au}\right)^{-2}\text{ m s}^{-2}$. The mass production rate Q of sublimating molecules can be found using,

$$M a(r) = \zeta Q v_{\text{H}_2}, \quad (1)$$

where M is the mass of the body, v_{H_2} is the velocity of the outgassing H₂, and ζ represents the fraction of outgassing momentum that is imparted in the anti-solar direction. v_{H_2} is found from $\left(\frac{8}{\pi}k_B T_{\text{H}_2}/m_{\text{H}_2}\right)^{1/2}$, where T_{H_2} is the temperature of outflowing H₂ and m_{H_2} is the H₂ mass. As discussed in more detail subsequently, we assume T_{H_2} is comparable to or lower than the surface temperature of the body, reflecting full or partial thermalization as H₂ escapes. Assuming an ellipsoidal shape, we solve for the *instantaneous* H₂ production rate needed to power the non-gravitational acceleration, $\dot{N}_{\text{H}_2,\text{accel}}$ (molecules s⁻¹):

$$\dot{N}_{\text{H}_2,\text{accel}} = \left(\frac{4}{3} \pi r_a r_b r_c \rho_{\text{Bulk}} a \right) / \left(\zeta m_{\text{H}_2} v_{\text{H}_2} \right), \quad (2)$$

where r_a , r_b , and r_c are the semi axes of the ellipsoid and ρ_{Bulk} is the density. The *total* number of required H₂ molecules $N_{H_2,accel}$ is found by integrating $\dot{N}_{H_2,accel}$ over time during the trajectory. Note that we only integrate over the portion of the trajectory during which astrometric measurements of the object were obtained, e.g. between 1.2–2.8 au, denoted by times t_i and t_f :

$$N_{H_2,accel} = \int_{t_i}^{t_f} \dot{N}_{H_2,accel}(\tau) d\tau. \quad (3)$$

To evaluate the feasibility of our hypothesis, we compare this with the number of H₂ molecules contained within a volumetric, ellipsoidal shell with a finite thickness d . To do so we first solve for the volumetric density of H₂ (molecules cm⁻³) within the body:

$$n_{H_2} = \frac{\rho_{Bulk} X_{H_2O/dust} X_{H_2/H_2O}}{m_{H_2O}}, \quad (4)$$

where $X_{H_2O/dust}$ is the H₂O:dust mass ratio, X_{H_2/H_2O} is the H₂:H₂O number ratio, and m_{H_2O} is the mass of H₂O. The RHS of Equation 4 is multiplied by the shell volume to calculate the total number of molecules in the outgassing shell, $N_{H_2,shell}$,

$$N_{H_2,shell} = X_{H_2O/dust} X_{H_2/H_2O} \frac{4\pi}{3} \left(\frac{\rho_{Bulk}}{m_{H_2O}} \right) \left(r_a r_b r_c - (r_a - d)(r_b - d)(r_c - d) \right). \quad (5)$$

With this treatment, we implicitly assume that the H₂ content within an entire ellipsoidal shell should ultimately be available for outgassing. At a given time we expect that outgassing will only occur from the illuminated surface; however, ‘Oumuamua was tumbling with a rotational period much shorter than the time in which its heliocentric distance changed substantially. Therefore,

over the trajectory the entire surface of the body should have been exposed to the Sun and subject to H₂ outgassing.

We adopt as our feasibility criterion the dimensionless quantity given by dividing Equation 5 by Equation 3:

$$N_{\text{H}_2, \text{shell}} / N_{\text{H}_2, \text{accel}} = X_{\text{H}_2\text{O}/\text{dust}} X_{\text{H}_2/\text{H}_2\text{O}} \left(\frac{m_{\text{H}_2}}{m_{\text{H}_2\text{O}}} \right) \left(1 - \frac{(r_a - d)(r_b - d)(r_c - d)}{r_a r_b r_c} \right) \left(v_{\text{H}_2} \zeta / \int_{t_i}^{t_f} a(\tau) d\tau \right). \quad (6)$$

When the fraction $N_{\text{H}_2, \text{shell}}/N_{\text{H}_2, \text{accel}} > 1$, the scenario is feasible: the number of H₂ molecules in the shell is sufficient to explain the non-gravitational acceleration. Note that this condition is related to the model feasibility starting around the time of detection (roughly 1 au post-perihelion). As discussed subsequently, pre-discovery outgassing might require a larger $N_{\text{H}_2, \text{shell}}$. In Equation 6, we assume that the velocity of the outgassing H₂ is independent of heliocentric distance. $N_{\text{H}_2, \text{shell}}/N_{\text{H}_2, \text{accel}}$ does not formally depend on ρ_{Bulk} . We assume a constant $X_{\text{H}_2/\text{H}_2\text{O}}$ of either 0.3 or 0.4, corresponding to an H₂ yield of 23–28% of the original H₂O content, as described in the main text. Other unconstrained parameters that influence $N_{\text{H}_2, \text{shell}}/N_{\text{H}_2, \text{accel}}$ are the outgassing depth, the size of the body, the outgassing temperature, the outflowing gas geometry (approximated by ζ), and the mass ratio $X_{\text{H}_2\text{O}/\text{dust}}$. The size of the body is degenerate with geometric albedo (p), and we explore a range of albedos from 0.05–0.9. The axis lengths of the ellipsoid (r_a , r_b , and r_c) are found by rescaling the dimensions found for an albedo of 0.1 (115 x 111 x 19 meters) by a factor of $\sqrt{0.1/p}$ ²³. We also model a range of outgassing depths from 100–800 cm to explore the depth required to explain the magnitude of observed non-gravitational acceleration. Note that for

high albedos, the nominal outgassing depth can be larger than the minor axis r_c ; these cases are unphysical and result in the blank region of parameter space shown in Figure 1.

For T_{H_2} and $X_{\text{H}_2\text{O}/\text{dust}}$, we evaluate two end member cases. For the first, less conservative case we assume an outgassing temperature of 140 K and a $\text{H}_2\text{O}/\text{dust}$ mass ratio of 3:1. This temperature assumes that the escaping H_2 molecules are thermalized as they leave the surface. While higher surface temperatures are possible (Figure 2), the water matrix will begin to sublime somewhat above 140 K. A water:dust mass ratio of 3:1 was found to be the best fit to an outgassing model of ‘Oumuamua by ⁷. For the second, more conservative model we assume a lower outgassing temperature of 100 K, representative of a scenario in which the escaping H_2 is not fully thermalized with the surface layers of the body; and a lower $\text{H}_2\text{O}/\text{dust}$ mass ratio of 1:1. The second model is conservative in that both the lower temperature and the lower $X_{\text{H}_2\text{O}/\text{dust}}$ result in a lower $N_{\text{H}_2,\text{shell}}$ for a given albedo and outgassing depth.

We also test two cases for the outflow geometry. For a fully collimated outflow, all momentum from the outgassing H_2 is imparted in the anti-solar direction, corresponding to $\zeta = 1$. For an entirely isotropic hemispherical outflow, half of the momentum is anti-solar, corresponding to $\zeta = 0.5$. In reality, the outflow geometry is likely in between these cases. Note that in addition to the parameters explored here, a momentum contribution from H_2O sublimation would further expand the allowable parameter space compared to what is shown in Figure 1.

For reference, we calculate the the H_2 mass production rate Q at 1.25 au. Assuming an outgassing temperature of 100 K and $\zeta=0.75$, the mass loss rate ranges from $\sim 10\text{--}800 \text{ g s}^{-1}$ for

the high- and low-albedo extremes, respectively. This is lower than previous estimates of the H₂O mass loss rate required to power the non-gravitational acceleration^{7,8}, due to a combination of (i) a higher gas velocity due to the smaller mass of H₂ compared to H₂O, and (ii) different assumptions about the size of the body.

Thermal model In this section we describe our numerical thermodynamic model of the interior temperature of ‘Oumuamau. This calculation is similar to the numerical experiments published by³ and³⁶. The absorbed solar flux, Φ_{\odot} , along the trajectory is,

$$\Phi_{\odot}(t) = \left(\frac{\xi L_{\odot}}{4\pi R(t)^2} \right) (1 - p), \quad (7)$$

where p is the albedo, $R(t)$ is the time-dependent heliocentric distance and $\xi = 0.25$ is the average projected surface area⁴⁰. We adopt $p=0.1$ as the fiducial albedo; the resulting temperature profile is only weakly sensitive to the choice of albedo, and a higher albedo for the thermal model does not affect our conclusions. We solve the radial temperature profile by solving the heat conduction equation in cylindrical coordinates,

$$\frac{dT}{dt} = \frac{\kappa}{\rho_{Bulk} c_P} \frac{1}{r} \frac{\partial}{\partial r} \left(r \frac{\partial T}{\partial r} \right), \quad (8)$$

for the temperature T . In Equation 8, κ is the thermal conductivity, c_P is the specific heat capacity, and r is the depth. We implement an iterative scheme that uses a second order Newton-Raphson technique to solve for the temperature at the surface, T_{Surf} . This T_{Surf} must balance (i) the absorption of solar flux ($\Phi_{\odot}(t)$), (ii) the heating of the surface element material ($c_P \rho_{Bulk} \Delta r \Delta T_{\text{Surf}}$) (iii) the reradiation from the surface ($\epsilon \sigma T_{\text{Surf}}^4$), and (iv) diffusion of heat from the surface into the

interior ($\kappa \frac{dT}{dr}_{r=0}$). The outer boundary condition is given by,

$$\Phi_{\odot}(t) - \epsilon\sigma T_{\text{Surf}}^4 - \kappa \frac{dT}{dr}_{r=0} - c_P \rho_{\text{Bulk}} \Delta r \Delta T_{\text{Surf}} = 0. \quad (9)$$

In Equation 9, $\epsilon \sim 0.95$ is the emissivity and σ is the Stefan-Boltzmann constant. Because the thermal properties of ‘Oumuamua are unconstrained, we assume a bulk density $\rho_{\text{Bulk}} = 0.5 \text{ g cm}^{-3}$, typical of cometary nuclei ⁴¹, and a specific heat capacity of $c_P = 2000 \text{ J kg}^{-1} \text{ K}^{-1}$ typical for cometary materials and ices. We produce thermal models for $\kappa = 10^{-2} \text{ W K}^{-1} \text{ m}^{-1}$ and $\kappa = 10^{-1} \text{ W K}^{-1} \text{ m}^{-1}$ ⁴².

Our thermal model implies that H_2 outgassing may be possible well before perihelion. Specifically, temperatures $> 15 \text{ K}$ are achieved down to depths of ~ 2 and ~ 8 meters prior to perihelion for thermal conductivities of $\kappa = 10^{-2}$ and $\kappa = 10^{-1} \text{ W K}^{-1} \text{ m}$, respectively (Figure 3). This raises the question of whether it is sufficient to explain ‘Oumuamua’s non-gravitational acceleration only during the portion of the trajectory from 1–3 au post-perihelion when astrometric measurements were obtained. However, there are major challenges associated with projecting any model prior to the observable apparition. It is not obvious that the non-gravitational acceleration, which was required to remove long-term trends from 76 days of astrometry⁷, can be extrapolated to the entire trajectory. Other equally plausible scenarios exist, including that (i) the presence of a low-conductivity regolith delayed the propagation of warming until post-perihelion^{3,36}; or (ii) the body experienced ice sublimation around perihelion, leading to changes in its size and/or shape⁹, with the implication that the original reservoir of H_2 (and H_2O) available to power an outgassing recoil was larger than what would be inferred from the observations starting at 1.2 au post-perihelion.

Given these uncertainties, we only consider outgassing between $\sim 1\text{--}3$ au when there are constraints on ‘Oumuamua’s dimensions and non-gravitational acceleration. Still, we note that for some parameter space (Figure 1), the outgassing shell contains factors of a few more H_2 molecules than is necessary to explain the non-gravitational acceleration from 1–3 au. It therefore remains plausible that H_2 outgassing was ongoing prior to perihelion.

1. Williams, G. V. *et al.* Minor Planets 2017 SN_33 and 2017 U1. *Central Bureau Electronic Telegrams* **4450**, 1 (2017).
2. Meech, K. J. *et al.* A brief visit from a red and extremely elongated interstellar asteroid. *Nature* **552**, 378–381 (2017).
3. Fitzsimmons, A. *et al.* Spectroscopy and thermal modelling of the first interstellar object 1I/2017 U1 ‘Oumuamua. *Nature Astronomy* **2**, 133–137 (2018).
4. Jewitt, D. *et al.* Interstellar Interloper 1I/2017 U1: Observations from the NOT and WIYN Telescopes. *Astrophys. J. L.* **850**, L36 (2017).
5. Ye, Q.-Z., Zhang, Q., Kelley, M. S. P. & Brown, P. G. 1I/2017 U1 (“Oumuamua) is Hot: Imaging, Spectroscopy, and Search of Meteor Activity. *Astrophys. J. L.* **851**, L5 (2017).
6. Trilling, D. E. *et al.* Spitzer Observations of Interstellar Object 1I/“Oumuamua. *Astron. J.* **156**, 261 (2018).
7. Micheli, M. *et al.* Non-gravitational acceleration in the trajectory of 1I/2017 U1 (‘Oumuamua). *Nature* **559**, 223–226 (2018).

8. Jewitt, D. & Seligman, D. Z. The Interstellar Interlopers. *arXiv e-prints* arXiv:2209.08182 (2022).
9. Seligman, D. & Laughlin, G. Evidence that 1I/2017 U1 ('Oumuamua) was Composed of Molecular Hydrogen Ice. *Astrophys. J. L.* **896**, L8 (2020).
10. Levine, W. G., Cabot, S. H. C., Seligman, D. & Laughlin, G. Constraints on the Occurrence of 'Oumuamua-Like Objects. *Astrophys. J.* **922**, 39 (2021).
11. Desch, S. J. & Jackson, A. P. 1I/'oumuamua as an n₂ ice fragment of an exo-pluto surface ii: Generation of n₂ ice fragments and the origin of 'oumuamua. *Journal of Geophysical Research: Planets* e2020JE006807 (2021).
12. Seligman, D. Z., Levine, W. G., Cabot, S. H. C., Laughlin, G. & Meech, K. On the Spin Dynamics of Elongated Minor Bodies with Applications to a Possible Solar System Analogue Composition for 'Oumuamua. *Astrophys. J.* **920**, 28 (2021).
13. Moro-Martín, A. Could 1I/'oumuamua be an icy fractal aggregate? *Astrophys. J. L.* **872**, L32 (2019).
14. Sekanina, Z. 1I/'Oumuamua and the Problem of Survival of Oort Cloud Comets Near the Sun. *arXiv e-prints* arXiv:1903.06300 (2019).
15. Luu, J. X., Flekkøy, E. G. & Toussaint, R. 'Oumuamua as a Cometary Fractal Aggregate: The "Dust Bunny" Model. *Astrophys. J. L.* **900**, L22 (2020).

16. Bar-Nun, A., Herman, G., Rappaport, M. L. & Mekler, Y. Ejection of H₂O, O₂, H₂ and H from water ice by 0.5-6 keV H⁺ and Ne⁺ ion bombardment. *Surface Science* **150**, 143–156 (1985).
17. Sandford, S. A. & Allamandola, L. J. H₂ in Interstellar and Extragalactic Ices: Infrared Characteristics, Ultraviolet Production, and Implications. *Astrophys. J. L.* **409**, L65 (1993).
18. Watanabe, N., Horii, T. & Kouchi, A. Measurements of D₂ Yields from Amorphous D₂O Ice by Ultraviolet Irradiation at 12 K. *Astrophys. J.* **541**, 772–778 (2000).
19. Grieves, G. A. & Orlando, T. M. The importance of pores in the electron stimulated production of D₂ and O₂ in low temperature ice. *Surface Science* **593**, 180–186 (2005).
20. Zheng, W., Jewitt, D. & Kaiser, R. I. Formation of Hydrogen, Oxygen, and Hydrogen Peroxide in Electron-irradiated Crystalline Water Ice. *Astrophys. J.* **639**, 534–548 (2006).
21. Zheng, W., Jewitt, D. & Kaiser, R. I. Temperature Dependence of the Formation of Hydrogen, Oxygen, and Hydrogen Peroxide in Electron-Irradiated Crystalline Water Ice. *Astrophys. J.* **648**, 753–761 (2006).
22. Zheng, W., Jewitt, D. & Kaiser, R. I. Electron irradiation of crystalline and amorphous D₂O ice. *Chemical Physics Letters* **435**, 289–294 (2007).
23. Mashchenko, S. Modelling the light curve of ‘Oumuamua: evidence for torque and disc-like shape. *Mon. Not. R. Astron. Soc.* **489**, 3003–3021 (2019).

24. Mamajek, E. Kinematics of the Interstellar Vagabond 1I/'Oumuamua (A/2017 U1). *Research Notes of the American Astronomical Society* **1**, 21 (2017).
25. Hallatt, T. & Wiegert, P. The Dynamics of Interstellar Asteroids and Comets within the Galaxy: An Assessment of Local Candidate Source Regions for 1I/'Oumuamua and 2I/Borisov. *Astron. J.* **159**, 147 (2020).
26. Park, R. S., Pisano, D. J., Lazio, T. J. W., Chodas, P. W. & Naidu, S. P. Search for OH 18 cm Radio Emission from 1I/2017 U1 with the Green Bank Telescope. *Astron. J.* **155**, 185 (2018).
1803.10187.
27. Maggiolo, R. *et al.* The Effect of Cosmic Rays on Cometary Nuclei. II. Impact on Ice Composition and Structure. *Astrophys. J.* **901**, 136 (2020).
28. Gronoff, G. *et al.* The Effect of Cosmic Rays on Cometary Nuclei. I. Dose Deposition. *Astrophys. J.* **890**, 89 (2020).
29. Derenne, S. & Robert, F. Model of molecular structure of the insoluble organic matter isolated from Murchison meteorite. *Meteoritics and Planetary Science* **45**, 1461–1475 (2010).
30. Rubin, M. *et al.* Elemental and molecular abundances in comet 67P/Churyumov-Gerasimenko. *Mon. Not. R. Astron. Soc.* **489**, 594–607 (2019).
31. Laufer, D., Kochavi, E. & Bar-Nun, A. Structure and dynamics of amorphous water ice. *Physical Review B: Solid State* **36**, 9219–9227 (1987).

32. Bar-Nun, A. & Prialnik, D. The Possible Formation of a Hydrogen Coma around Comets at Large Heliocentric Distances. *Astrophys. J. L.* **324**, L31 (1988).
33. Gundlach, B. & Blum, J. Outgassing of icy bodies in the Solar System - II: Heat transport in dry, porous surface dust layers. *Icarus* **219**, 618–629 (2012).
34. Prialnik, D. & Jewitt, D. Amorphous ice in comets: evidence and consequences. *arXiv e-prints* arXiv:2209.05907 (2022).
35. Sekanina, Z. Outgassing As Trigger of 1I/‘Oumuamua’s Nongravitational Acceleration: Could This Hypothesis Work at All? *arXiv e-prints* arXiv:1905.00935 (2019).
36. Seligman, D. & Laughlin, G. The Feasibility and Benefits of In Situ Exploration of ‘Oumuamua-like Objects. *Astron. J.* **155**, 217 (2018).
37. Fink, U. A taxonomic survey of comet composition 1985-2004 using CCD spectroscopy. *Icarus* **201**, 311–334 (2009).
38. Newburn, R. L. & Spinrad, H. Spectrophotometry of seventeen comets. II - The continuum. *Astron. J.* **90**, 2591–2608 (1985).
39. Stern, S. Ism-induced erosion and gas-dynamical drag in the oort cloud. *Icarus* **84**, 447–466 (1990).
40. Meltzer, B. Shadow Area of Convex Bodies. *Nature* **163**, 220 (1949).

41. Britt, D. T., Consolmagno, G. J. & Merline, W. J. Small Body Density and Porosity: New Data, New Insights. In Mackwell, S. & Stansbery, E. (eds.) *37th Annual Lunar and Planetary Science Conference*, Lunar and Planetary Science Conference, 2214 (2006).
42. Steckloff, J. K. *et al.* The sublimative evolution of (486958) Arrokoth. *Icarus* **356**, 113998 (2021).

Acknowledgements We thank Dave Jewitt, Mike Brown, Davide Farnocchia, Karen Meech, Dong Lai, Alessandro Morbidelli, Luke Kelley, Jonathan Lunine and Samantha Trumbo for useful conversations and suggestions. We thank the scientific editor, Leslie Sage, and the two anonymous reviewers for insightful comments and constructive suggestions that greatly strengthened the scientific content of this manuscript. DZS acknowledges financial support from the National Science Foundation Grant No. AST-17152, NASA Grant No. 80NSSC19K0444 and NASA Contract NNX17AL71A from the NASA Goddard Spaceflight Center. J.B.B. acknowledges support from NASA through the NASA Hubble Fellowship grant HST-HF2-51429.001-A awarded by the Space Telescope Science Institute, which is operated by the Association of Universities for Research in Astronomy, Incorporated, under NASA contract NAS5-26555.

Author contributions J. B. B. performed the H₂ budget modeling and led the writing of the manuscript. D. Z. S. performed the thermal modeling and contributed to the manuscript text.

Data and Code availability The datasets generated and analysed during the current study are available on GitHub at https://github.com/bergnerjb/Oumuamua_H2. All code used for this manuscript is available on GitHub at https://github.com/bergnerjb/Oumuamua_H2.

Competing Interests The authors declare that they have no competing financial interests.

Correspondence Correspondence and requests for materials should be addressed to J. B. B. (jbergner@berkeley.edu).